# Transgenerational Effects of Di-(2-ethylhexyl) Phthalate on Testicular Germ Cell Associations and Spermatogonial Stem Cells in Mice 1

Authors: Doyle, Timothy J., Bowman, Jennifer L., Windell, Veronica L., McLean, Derek J., and Kim, Kwan Hee

Source: Biology of Reproduction, 88(5)

Published By: Society for the Study of Reproduction

URL: https://doi.org/10.1095/biolreprod.112.106104

BIOLOGY OF REPRODUCTION (2013) **88**(5):112, 1–15
Published online before print 27 March 2013.
DOI 10.1095/biolreprod.112.106104

# Transgenerational Effects of Di-(2-ethylhexyl) Phthalate on Testicular Germ Cell Associations and Spermatogonial Stem Cells in Mice[1]

**Timothy J. Doyle,[3,5] Jennifer L. Bowman,[3,5] Veronica L. Windell,[3,5] Derek J. McLean,[4,5] and Kwan Hee Kim[2,3,5]**

[3]*School of Molecular Biosciences, Washington State University, Pullman, Washington*
[4]*Department of Animal Sciences, Washington State University, Pullman, Washington*
[5]*Center for Reproductive Biology, Washington State University, Pullman, Washington*

## ABSTRACT

**Recent evidence has linked human phthalate exposure to abnormal reproductive and hormonal effects. Phthalates are plasticizers that confer flexibility and transparency to plastics, but they readily contaminate the body and the environment. In this study, timed pregnant CD1 outbred mice were treated with di-(2-ethylhexyl) phthalate (DEHP) from Embryonic Day 7 (E7) to E14. The subsequent generation (F1) offspring were then bred to produce the F2, F3, and F4 offspring, without any further DEHP treatment. This exposure scheme disrupted testicular germ cell association and decreased sperm count and motility in F1 to F4 offspring. By spermatogonial transplantation techniques, the exposure scheme also disrupted spermatogonial stem cell (SSC) function of F3 offspring. The W/W$^{V}$ recipient testes transplanted with F3 offspring germ cells from the DEHP-treated group had a dramatically lower percentage of donor germ cell-derived spermatogenic recovery in seminiferous tubules when compared to the recipient testes transplanted with CD1 control germ cells. Further characterization showed that the major block of donor germ cell-derived spermatogenesis was before the appearance of undifferentiated spermatogonia. Interestingly, the testes transplanted with the F3 offspring germ cells from the DEHP-treated group, when regenerated, replicated testis morphology similar to that observed in the testes from the F1 to F3 offspring of the DEHP-treated group, suggesting that the germ cell disorganization phenotype originates from the stem cells of F3 offspring. In conclusion, embryonic exposure to DEHP was found to disrupt testicular germ cell organization and SSC function in a transgenerational manner.**

*DEHP, environmental contaminants and toxicants, male germ cells, spermatogenesis, spermatogonial stem cells, testis, transgenerational*

## INTRODUCTION

Plastics are an important component of the world we live in today, with their production reaching 245 million tons in 2006 and increasing each year [1]. One class of chemical component of plastics is phthalate plasticizers that confer flexibility and transparency to plastics. Phthalate esters are found in a wide range of consumer products, from food packaging and personal care products to medical devices and pharmaceuticals. Phthalate esters are not linked covalently to the plastics, so they are highly susceptible to leaching into the environment. Of the different phthalate esters, the most abundantly produced is di-(2-ethylhexyl) phthalate (DEHP), manufactured at an annual rate of 2 million tons [1].

Humans and animals are exposed to phthalates via multiple routes, including ingestion, inhalation, absorption by dermal contact, and the parenteral route [2]. In the body, DEHP is metabolized into its active monoesters in the intestines and liver by esterases and further degraded to more water-soluble metabolites for excretion. Seven phthalate metabolites in urine samples were measured from 2540 individuals participating in the National Health and Nutrition Examination Survey of 1999–2000 [3]. Mono-ethyl phthalate was in all samples, mono-butyl phthalate in 99% of the samples, and mono-ethylhexyl phthalate (MEHP) in 78% of the samples. The median phthalate exposure in adults was estimated to be 8.2 μg/kg/day and in toddlers 25.8 μg/kg/day [2]. Women were found to have two to four times higher levels of phthalate exposure compared to men [3]. Younger children have a significantly higher exposure than older children [4]. Infants around 1 yr of age were found to be particularly at high risk because of their behavioral patterns of feeding and chewing and of crawling on carpets inhaling phthalate dust [2]. Moreover, the National Toxicity Program had the most serious concern for patients in the neonatal intensive care unit, with an exposure rate as high as 6 mg/kg/day [2]. These neonates undergo blood transfusions and extracorporeal membrane oxygenation, medical procedures that involve DEHP-containing polyvinylchloride medical devices.

Human phthalate exposure is becoming an increasing public health concern, with researchers linking phthalates to a reduction in sperm motility and chromatin damage [5], disruption of fetal germ cell development [6], disruption of Leydig cell development and testosterone levels [7, 8], and a reduction in anogenital distance (AGD) [9, 10]. The prevailing thought is that phthalates can induce testicular dysgenesis syndrome (TDS), which originates from disrupted development of fetal testes, manifesting postnatally as cryptorchidism, impaired spermatogenesis, low sperm count and damage, hypospadias, and/or testicular cancer [11].

Compared to rather limited information on the effects of phthalates on humans, phthalates (DEHP and di(n-butyl) phthalate) have been extensively studied in rodents. Similar to humans, phthalates are considered antiandrogens, causing TDS-like syndrome in rodents, but not by interacting with the androgen receptor [12–14]. For example, in utero and

[1]Supported in part by NIH grant ES019836 (to K.H.K.) from the National Institute of Environmental Health Sciences (NIEHS).
[2]Correspondence: Kwan Hee Kim, School of Molecular Biosciences, 1715 NE S. Fairway Rd., Washington State University, Pullman, WA 99164. E-mail: khkim@wsu.edu

Received: 8 November 2012.
First Decision: 6 December 2012.
Accepted: 21 March 2013.

eISSN: 1529-7268 http://www.biolreprod.org
ISSN: 0006-3363

lactational exposure [15–17] or in vitro exposure [18] has resulted in abnormal Leydig cell clusters and decreased testosterone levels. Lowered testosterone levels are thought to account for reduction in AGD, incomplete preputial separation, increased areola/nipple retention, cryptorchidism, penile malformations, sperm count and sexual inactivity, abnormal testicular morphology, and inhibition of sexually dimorphic central nervous system development [12–14, 19, 20]. In contrast, for some phthalate responses, the mechanism of how phthalate acts may be different in rats from that in the mouse. For example, in utero exposure or in vitro neonatal exposure of phthalates has increased the number of multinucleated gonocytes in rats [17, 21] and mice [22], but this response has not been linked to lowered fetal testosterone levels in mice [22, 23], whereas associations between lowered testosterone levels and multinucleated gonocytes has been made in rats [17, 21, 24]. Additionally, the effect of phthalates on testosterone levels may vary with developmental age [21].

Recently, in utero exposure to compounds including vinclozolin, bisphenol A, dioxin, polycyclic aromatic hydrocarbon benzo(a)pyrene, polychlorinated biphenyls, a mixture of pesticides (permethrin and the insect repellent *N,N*-Diethyl-*meta*-toluamide), a mixture of plastics (bisphenol A and phthalates), dioxin and a hydrocarbon mixture, and high-energy diet have been found to induce reproductive disorders in a transgenerational manner in rats [25–28] and in mice [29–32]. Even in human populations, there is accumulating evidence of transgenerational nutritional or endocrine disruptor effects on the F2 offspring [33–36]. For example, Dutch famine in 1944–1945 has been associated with increased F2 offspring neonatal adiposity and poor health in later life [34]. Similarly, both grandsons and granddaughters of women exposed in utero to diethylstilbestrol between the late 1940s and early 1970s have a higher incidence of birth defects [36], grandsons have an increased occurrence of hypospadias [33], and preliminary data on the granddaughters suggest a higher incident of ovarian cancer [35].

We sought to determine if maternal exposure to DEHP from Embryonic Day E7 (E7) to E14 of pregnancy exerts transgenerational effects on the testis and spermatogonial stem cells (SSCs) of the offspring. The treatment window was chosen to include the time of primordial germ cell migration around E8.5, global DNA methylation pattern changes, DNA demethylation in both male and female germ cells around E10.5–E13.5 and remethylation in male germ cells around E14.5, and sex determination at E12.5 [37]. Female remethylation occurs in a broader range of time during embryo and neonatal development [37]. This window of treatment is thought to be critical for epigenome changes that can be transmitted to multiple generations. We found that germ cell associations in the testis were disturbed and sperm counts and motility declined in multiple generations, and, importantly, the SSC function of F3 offspring was impaired in a transgenerational manner.

## MATERIALS AND METHODS

### Animals

Crl:CD1(ICR) (CD1) outbred mice were obtained from Charles River Laboratories (Wilmington, MA) or an in-house vivarium. WBB6F1/J-Kit$^{W}$/Kit$^{W\text{-}V}$ (W/W$^{v}$) mice were obtained from an in house vivarium or purchased from Jackson Laboratories (Bar Harbor, ME). Animal experimentation and procedures were approved by the Washington State University Institutional Animal Care and Use Committee. Animals were treated humanely in accordance with the standards of care outlined by the NIH *Guide for the Care and Use of Laboratory Animals*.

### DEHP Treatment and Breeding to Obtain F1–F4 Offspring

Postnatal Day (P) 60–64 (P60–64) CD1 females were continuously paired with age-matched CD1 males for generating offspring. Females were examined twice daily for the presence of vaginal plugs, the presence of which was set as E0. Twenty vaginal plug-positive dams were gavaged from E7 to E14 of gestation with DEHP (500 mg/kg body weight/day) (Sigma-Aldrich Chemical Co., St. Louis, MO) in 200 μl of superrefined corn oil (Croda Inc., Edison, NJ) (DEHP-treated group) or gavaged with 200 μl of corn oil alone (vehicle control group). A review [38] citing the comparison of the measurement of phthalate metabolites in amniotic fluids in rodents [39] and humans [3] indicated that the dose range including a 300 mg/kg/day dose in animal studies is relevant to understanding TDS in humans and the animal dosages are not excessively high as originally thought. The treated gestating dams were considered the F0 generation (F0) dams, and the pups born from the F0 dams were labeled as the F1 generation (F1) offspring. The F1 offspring were used in three breeding paradigms to follow inheritance through the maternal, paternal, and double-cross lines. Paternal lines were generated by breeding males from the treated groups (both DEHP-treated and vehicle control) with age-matched nontreated CD1 females. Maternal lines were generated by breeding females from the treated groups with age-matched nontreated CD1 males. For the double-cross lines, males were bred to females, both from the same treated group. Each paradigm was repeated to produce F2 to F4 offspring. No inbreeding was performed.

### Embryonic Survival and Weaning Rates

The number of implantation sites on uterine horns, representing the number of embryos embedded in the uterine wall, was determined from the F0 dams at the day of pup weaning using a stereomicroscope (Leica MZ 9.5; Leica, Wetzlar, Germany). The litter size was noted on P1, the body weights were measured at P10, and the number of pups successfully reared to weaning was noted on the day of weaning (P21).

### Neonatal and Pubertal Period Analysis

Anogenital distance (AGD) was measured on neonatal pups at P1 by two independent researchers. The distance from the urethral opening to the ventral opening of the anus was measured in millimeters under a stereomicroscope (Leica MZ 9.5). Pups at P10 were anesthetized and nipple positions were determined by measuring the distance of each nipple to the umbilical stump. The nipples were numbered in a pattern beginning with the right foremost cranial nipple labeled nipple 1, the right axillary nipple labeled nipple 2, and continuing down to the rightmost caudal nipple labeled nipple 5. The order was reversed on the left side with the leftmost caudal nipple labeled nipple 6, the inguinal nipple labeled nipple 8, and continuing up to the left foremost cranial nipple, labeled nipple 10. Pubertal onset occurs around the time when the penis detaches from the prepuce in male pups and was determined by retracting the prepuce manually using gentle pressure beginning at P20 onward.

### Testicular Tissue Collection and Determination of Testicular Abnormalities

Male mice were killed at P30 and P120 for F1–F4 generations and P360 for F4 generation and their testes were collected, fixed in Bouin solution for 1–5 h or 4% paraformaldehyde (PFA) with 0.25% glutaraldehyde for 4–6 h at 4°C, and embedded in paraffin. Four-micrometer-thick serial sections were cut and mounted on poly-L-lysine slides. To examine testicular morphology, sections were deparaffinized, stained with hematoxylin and eosin, and examined using a Leitz DMRB microscope (Leica). Digital images were obtained by using a Magnafire digital camera (Optronics, Goleta, CA). To determine the percentage of abnormal tubules present in the testes, tubules having moderate to severe germ cell disorganization and the total number of tubules were counted in testicular sections. To obtain good sampling across the entire testis, a minimum of four sections spaced 50 μm apart were counted. This was repeated for at least three animals.

### Detection of Apoptosis by TUNEL Assay

Testicular sections fixed in 4% PFA with 0.25% glutaraldehyde were used for the detection of apoptotic cells by TUNEL assay (Promega Corporation, Madison, WI). This assay identifies fragmented DNA by the terminal deoxynucleotidyl transferase (TdT)-mediated incorporation of fluorescein-12-dUTP at the 3′ hydroxyl end of DNA. For a positive control, tissue sections were pretreated with deoxyribonuclease I, and for a negative control, tissue sections were not incubated with TdT. Apoptotic cells were visualized by green

fluorescence using a microscope. Tubules with four or more apoptotic cells (representing apoptotic tubules) and the total number of tubules were counted to quantify the results.

### Sperm Count and Determination of Sperm Motility

Sperm was collected from the caudal epididymis of F1–F4 male offspring at P120. The excised epididymides were cut in 2-mm intervals (five cuts) and placed in F12 media (1 ml) containing 0.1% bovine serum albumin prewarmed to 37°C and incubated for 15 min to facilitate sperm transmigration from the epididymis. Fresh sperm were loaded into a hemacytometer and counted. Each chamber was counted twice and averaged. A prewarmed glass slide was loaded with fresh sperm, coverslipped, and examined by phase contrast light microscopy to determine sperm motility. Sperm motility was scored in five randomly chosen fields for two samples from each animal. The number of sperm exhibiting forward and progressive activity and the total number of sperm were counted to obtain the percentage sperm motility. Sperm clumps, detached heads, and free tails were not counted.

### Spermatogonial Transplantation

Three F3 male offspring at P24–P31 from the DEHP-treated group in the double-cross line provided the donor germ cells for spermatogonial transplantation. Germ cells from two age-matched untreated CD1 male mice served as controls. As described [40], the testes were detunicated, tubules were digested with enzymes, and single-cell suspensions were obtained. The donor germ cells were counted using a hemacytometer and resuspended at a concentration of $10^7$ cells/ml in minimal essential media α with 0.03% trypan blue dye (Invitrogen Corporation, Carlsbad, CA). Donor germ cells were transplanted into testes of at least three $W/W^V$ mice per donor animal. A small hole was made in the connective tissue enclosing the efferent ducts of the recipient mouse and a glass needle containing 7 μl (70 000 cells) of the donor germ cell suspension was inserted into the rete testis through the efferent ducts for the injection. After injection, the animals were allowed to recover for 70 days. By this time, all stages of germ cells, including meiotic and postmeiotic germ cells, were represented in the recipient tubules injected with control SSCs.

### Posttransplantation Recovery Analysis

The recipient $WW^V$ testicular tissues and noninjected $WW^V$ testicular tissues were fixed in Bouin solution for 2 h and embedded in paraffin, and 4-μm-thick serial sections were cut. To determine the donor-derived germ cell recovery, the tubules containing round or elongated spermatids, more than four sections separated by 50 μm per testis from at least three animals, were stained with hematoxylin and eosin and examined using a Leitz DMRB microscope, and digital images were obtained using a Magnafire digital camera. To further determine the germ cell types present in the recovered tubules, immunohistochemistry or immunofluorescence was performed using antibodies for DDX4, γH2AX, STRA8, and DMRT1.

### Immunohistochemistry and Immunofluorescence

For immunohistochemistry, after a sodium citrate antigen retrieval step, tissue sections were incubated overnight with rabbit anti-STRA8 peptide antibody (1:2500 dilution) or rabbit anti-DDX4 peptide antibody (1:300 dilution; Abcam, Cambridge, MA), washed in PBS, and incubated with biotinylated anti-rabbit IgG (1:300 dilution; Vector Laboratories, Burlingame, CA), followed by streptavidin-peroxidase reaction and incubation with 3,3′-diaminobenzidine tetrahydrochloride (Invitrogen Corporation). For immunofluorescence, the tissue sections were further permeabilized with 0.2% Triton X-100 in PBS for 45 min. The rabbit polyclonal anti-DMRT1 antibody (1:300 dilution) incubation was followed by anti-rabbit IgG conjugated to Alexafluor-555 (1:1000 dilution; Invitrogen Corporation) secondary antibody. The mouse monoclonal anti-γH2AX peptide antibody (1:750 dilution; Millipore Corporation, Billerica, MA) incubation was followed by the use of Mouse on Mouse Basic Kit (Vector). Coverslips were mounted with ProLong Gold antifade reagent with 4′,6-diamidino-2-phenylindole (Invitrogen Corporation) on sections and examined by fluorescent microscopy (Leitz DMRB microscope).

### Statistical Significance

Statistical significance was determined by a pooled *t*-test or one-way ANOVA, followed by pairwise comparison of the means using the Student *t* method (JMP 9; SAS Institute Inc., Cary, NC). The *P* value of $<0.05$ was considered significant. We made a note of *P* values between 0.05 and $<0.1$ in the text.

## RESULTS

### DEHP Effect on Embryo Survival and Weaning Rates in CD1 Outbred Mice

We established the effect of a 500 mg/kg/day dose of DEHP between E7 and E14 on the embryo survival of the CD1 outbred strain. This window of treatment for CD1 mice had not been conducted previously. The number of implantation sites and litter sizes were determined for the F0, F1, and F2 dams. We found that the E7–E14 exposure of DEHP did not significantly affect the number of implantation sites in the DEHP-treated F0 dams (Fig. 1A). This was expected, as the treatment started 7 days after implantation. However, the litter size of the DEHP-treated F0 dams compared to vehicle control dams was different at $P = 0.0667$, showing a trend of 17.2% decrease in the litter size for DEHP-treated F0 dams (Fig. 1B). After birth, there was no significant difference at $P < 0.05$ in the wean rate of F1 pups between the DEHP-treated dams ($n = 6$) and vehicle-treated dams ($n = 3$). The neonatal survival of F1 offspring was 100%. For F2 and F3 embryo and neonatal survival, there were no significant differences in the number of implantation sites, the litter size of dams, and the wean rate of pups between the DEHP-treated and vehicle-treated groups for the paternal, maternal, and double-cross lines at $P < 0.05$ (Table 1). Thus, the embryo survival rate returned to normal for F2 and F3 embryos, indicating that the embryo survival rate is not transgenerational.

### DEHP Effect on Anogenital Distance, Body Weight, Nipple Retention, and Pubertal Onset

Fetal and lactational DEHP exposure that includes late embryonic stage E16–E20 has been found to decrease male AGD and increase the incidence of males retaining nipples/areolas in rats [12–14]. To examine if mouse embryos exposed to DEHP from E7 to E14 have similar alterations, the AGD at P1 and nipple/areola retention at P10 were examined. The F1 male offspring at P1 from the DEHP-treated group exhibited a significant decrease ($P < 0.0001$) in AGD when compared to their vehicle control male counterpart (Fig. 1C) or nontreated control CD1 pups (data not shown). The average AGD for the vehicle control group was 1.90 mm and for the DEHP group was 1.67 mm at P1. Moreover, the body weights of F1 male offspring at P10 from the DEHP group were greater (average of 7.81 g) than those of the vehicle-treated group (average of 5.63 g) (Fig. 1D). Additionally, we detected alopecia/xerosis in 83.4% of F1 offspring in the DEHP group ($n = 31$), whereas no incident was observed for the control group ($n = 17$). However, the decrease in male AGDs, the increase in body weights, and the occurrence of alopecia/xerosis were not passed to F2 and F3 offspring from the maternal, paternal, and double-cross lines, evaluated on 21–43 male offspring for each breeding line/treatment group.

Supernumerary nipples were observed with a 16.1% frequency in F1 male pups at P10 from the DEHP-treated group ($n = 31$) compared to no supernumerary nipples in the vehicle-treated ($n = 17$) male pups. The retained nipples corresponded to nipple positions 3, 4, and 8 (as described in *Materials and Methods*). Examining the positions individually, 9.7% of pups had supernumerary nipples at both positions 3 and 4, and 12.9% of pups had supernumerary nipples at position 8. However, the incidence of retained nipples was not transmitted to F2 and F3 offspring males ($n = 21$–43) for any breeding line or treatment group.

To determine if DEHP exposure disrupted pubertal onset, the penis detachment from the prepuce was examined in males

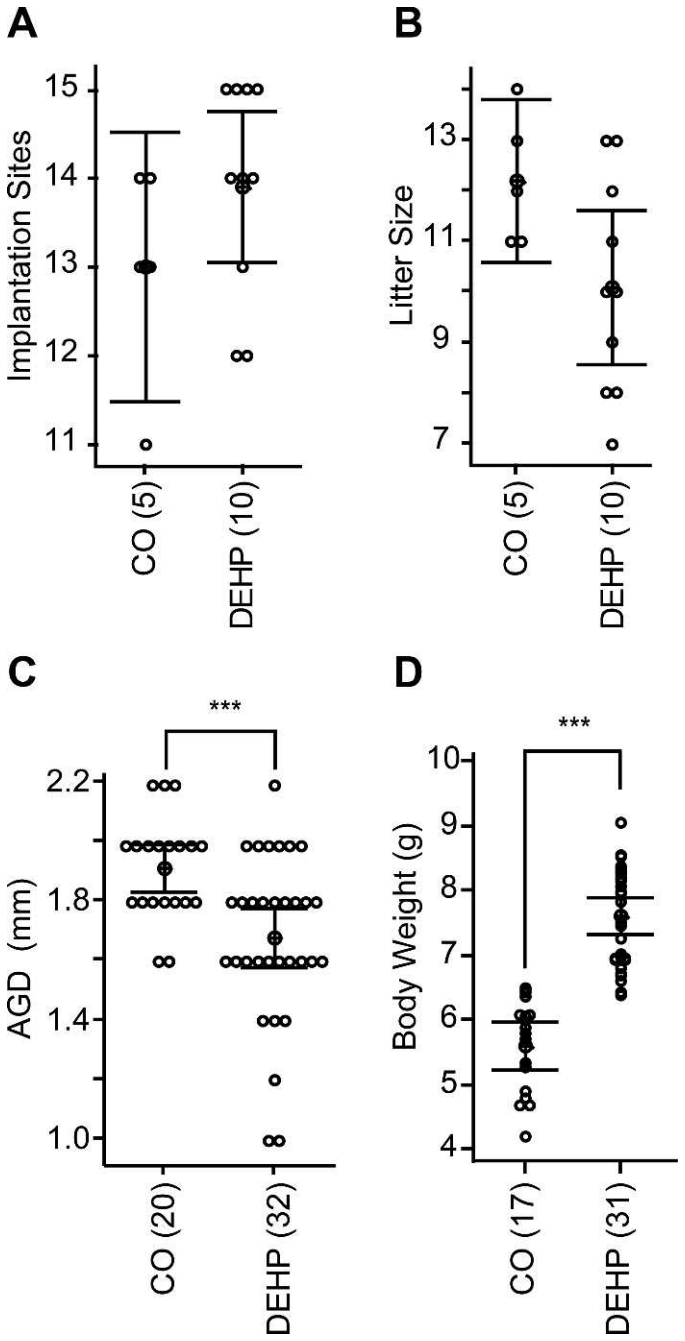


FIG. 1. Implantation sites and litter size for F0 dams, and AGDs and body weights of F1 offspring. Time-pregnant dams were treated with 500 mg/kg body weight/day DEHP or corn oil vehicle (CO) from E7 to E14. Individual value plots are shown for the number of implantation sites in F0 dams (**A**), the number of live pups born per litter for F0 dams (**B**), AGD measurements in millimeters for F1 pups at P1 (**C**), and the body weights in grams for F1 pups at P10 (**D**) from DEHP-treated or corn oil vehicle (CO)-treated dams. The number (n) in the parentheses indicates the number of dams for **A** and **B** and the number of male offspring for **C** and **D**. Values are mean ± SEM. Pooled *t*-tests were conducted for the control and DEHP values; ***$P < 0.001$, no asterisk indicates $P > 0.05$.

starting at P20. The average day of pubertal onset was P24.7 in the controls. The F1 offspring from DEHP-exposed dams had significantly delayed ($P < 0.05$) pubertal onset compared to controls (Fig. 2A). For F2 and F3 offspring, no significant difference at $P < 0.05$ was detected in pubertal onset between offspring of the DEHP-exposed and vehicle-exposed dams in the maternal line (Fig. 2, B and C). In contrast, the F2 and F3 offspring from the DEHP-exposed group had a significant delay ($P < 0.05$ to $< 0.0001$) in pubertal onset in the paternal and the double-cross lines compared to their vehicle counterparts (Fig. 2, B and C). These results show that DEHP decreased AGD, increased nipple retention, increased body weights, and caused alopecia/xerosis in F1 males, but these changes remained only in F1 offspring and did not transmit to F2 and F3 offspring. In contrast, male pubertal onset was delayed in F1 offspring and in F2 and F3 offspring of the paternal and double-cross lines, although the delay of pubertal onset was on average less than a day, relatively small for an outbred strain.

### *DEHP Increased Abnormal Seminiferous Tubule Morphology in F1–F4 Offspring*

Hematoxylin and eosin staining of testicular cross sections of F1–F3 offspring at P120 in the DEHP-treated group for the maternal, paternal, and double-cross lines revealed morphological abnormalities. The weights of testes from the control and DEHP group animals at P120 in the F2 and F3 generations were not significantly different at $P < 0.05$ (data not shown). For the vehicle control group, the testes of F1 (Fig. 3, A, C, and E), F2 (Fig. 4, A and E), F3 (Fig. 4, I and M), and F4 (Fig. 4, Q and R) offspring at P120 showed normal germ cell associations in the seminiferous tubules, with the different stages of the seminiferous epithelium cycle represented. In contrast, testes of F1 (Fig. 3, B, D, and F), F2 (Fig. 4, B–D and F–H), and F3 (Fig. 4, J–L and N–P) offspring at P120 from the DEHP-treated group in all three breeding lines had moderate to severe testicular abnormalities. On average, 27.1% (the range in the F2 generation was 18.8–34.2%, and in the F3 generation was 22.3–41.0%) of their seminiferous tubule sections had abnormalities in the F2 and F3 generations such that they could not be assigned to specific stages of the seminiferous epithelium. Tubules with moderate and severe abnormalities were easily identifiable, with one or more characteristics such as massive cell sloughing into the center of tubules (Fig. 3D and Fig. 4, D, N, and P), no lumen (Fig. 3, D and F, and Fig. 4, D, F, G, H, K, N, and P), a complete loss of germ cell organization (Fig. 3F and Fig. 4, F, G, H, K, and N), and large vacuoles from apparent bulk germ cell loss (arrow, Fig. 4, C, J and N). Also, a small number of tubules had areas where layers of germ cells were missing (oblong circle, Fig. 4, G, J, L, and O). The germ cells missing were round spermatids (Fig. 4, j‘ and l‘), leptotene (Fig. 4o‘) and pachytene spermatocytes (Fig. 4g‘). Likewise, testes of F4 offspring at P120 from the DEHP-treated group in the double-cross line (Fig. 4, S and T) had testicular morphologies similar to those from F1–F3 offspring from all three breeding lines.

To determine if the testicular abnormalities observed at P120 were progressively worse with aging, we examined the testes from F4 offspring at P360 in the double-cross line. Similar to testes from the P120 mice, seminiferous tubules of animals in the corn oil group had distinguishable stages of the seminiferous epithelium cycle (Fig. 5, A, D, and G). In contrast, testes from mice at P360 in the DEHP group showed abnormal testicular morphologies, much more severe than those observed at P120. Abnormal tubules showed large vacuoles (arrows, Fig. 5, E, F, and I), loss of germ cell organization (Fig. 5, B and H), and presence of multinucleated cells (Fig. 5, B and F, box and insets b‘ and f‘), which are thought to be precursors to cells that may become cancerous. Some severely abnormal tubules contained only a few layers of germ cells (Fig. 5I) and some had masses of unknown cell

TABLE 1. Implantation sites, litter size, and weaned rate for F1 and F2 dams.[a]

| Dam generation | Dam # (n) | Breeding scheme[b] | Treatment[c] | Implantation site (#) | Litter size (#) | Wean rate (%) |
|---|---|---|---|---|---|---|
| F1 | 5 | M | CO | 14.3 ± 0.5 | 13.9 ± 0.3 | 100.0 ± 0.0 |
| F1 | 4 | M | DEHP | 15.2 ± 0.3 | 14.9 ± 0.5 | 100.0 ± 0.0 |
| F1 | 4 | P | CO | 13.5 ± 0.7 | 13.2 ± 0.5 | 98.1 ± 1.9 |
| F1 | 5 | P | DEHP | 14.7 ± 0.3 | 14.3 ± 0.7 | 98.2 ± 1.8 |
| F1 | 4 | DC | CO | 16.1 ± 0.6 | 15.7 ± 0.7 | 98.2 ± 1.8 |
| F1 | 7 | DC | DEHP | 14.3 ± 0.9 | 13.9 ± 0.5 | 100.0 ± 0.0 |
| F2 | 8 | M | CO | 14.3 ± 0.3 | 14.0 ± 0.6 | 91.3 ± 8.8 |
| F2 | 8 | M | DEHP | 14.7 ± 0.7 | 14.3 ± .06 | 91.1 ± 8.9 |
| F2 | 6 | P | CO | 12.7 ± 0.3 | 12.3 ± 0.3 | 95.7 ± 3.0 |
| F2 | 8 | P | DEHP | 13.3 ± 0.3 | 13.0 ± 0.0 | 90.2 ± 6.0 |
| F2 | 5 | DC | CO | 12.7 ± 0.3 | 12.3 ± 0.3 | 96.9 ± 3.1 |
| F2 | 7 | DC | DEHP | 11.8 ± 0.5 | 11.5 ± 0.3 | 95.9 ± 4.1 |

[a] Pooled *t*-tests were conducted, and *P* values for the DEHP group to the control group is not significant at $P < 0.05$.
[b] M, maternal line; P, paternal line; DC, double-cross line.
[c] CO, corn oil vehicle control.

types (Fig. 5C). Epididymides of F4 offspring from the DEHP group showed round germ cells and multinucleated germ cells (Fig. 5, K and L), which should not be present in epididymides in normal condition.

To compare the frequency of testicular abnormalities, the percentages of moderate to severe abnormal seminiferous tubules were determined for the DEHP-treated and vehicle-treated groups. The testes from F1 offspring at P120 of the DEHP-exposed group had a statistically significant increase of 5.0-fold in the percentage of abnormal tubules compared to the testes from the vehicle control group (Fig. 6A). In F2 and F3 offspring at P120, the testes from the three breeding lines of the DEHP-exposed group were found to have significant changes in the percentage of abnormal tubules compared to their vehicle counterparts (Fig. 6, B and C), although the range of fold changes (2.8- to 3.2-fold) was lower than the 5.0-fold change observed for testes from F1 offspring.

In F4 offspring at P360, we found a 6.3-fold increase in abnormal tubules from the DEHP group compared to the vehicle control (Fig. 6D), which is more than the 2.8- to 3.2-fold increases observed for F2 and F3 offspring at P120, suggesting that testicular germ cell disorganization had increased with aging. F4 offspring at P360 had 66.6% of their tubules with moderate to severe testicular abnormalities compared to 27.1% of tubules in F2 and F3 offspring at P120. These results clearly show that the DEHP exposure of F0 dams induced testicular abnormalities in offspring of multiple generations (F1–F4), and that the frequency of testicular germ cell disorganization and abnormalities was higher in F1 compared to F2 and F3 generations and the frequency and severity increased with aging.

### *Germ Cell Apoptosis Did Not Contribute to F3 Offspring Phenotypes at P120*

To determine if germ cell apoptosis contributed to the germ cell loss and germ cell disorganization in F1–F3 offspring at P120, TUNEL analyses were performed on the testes derived

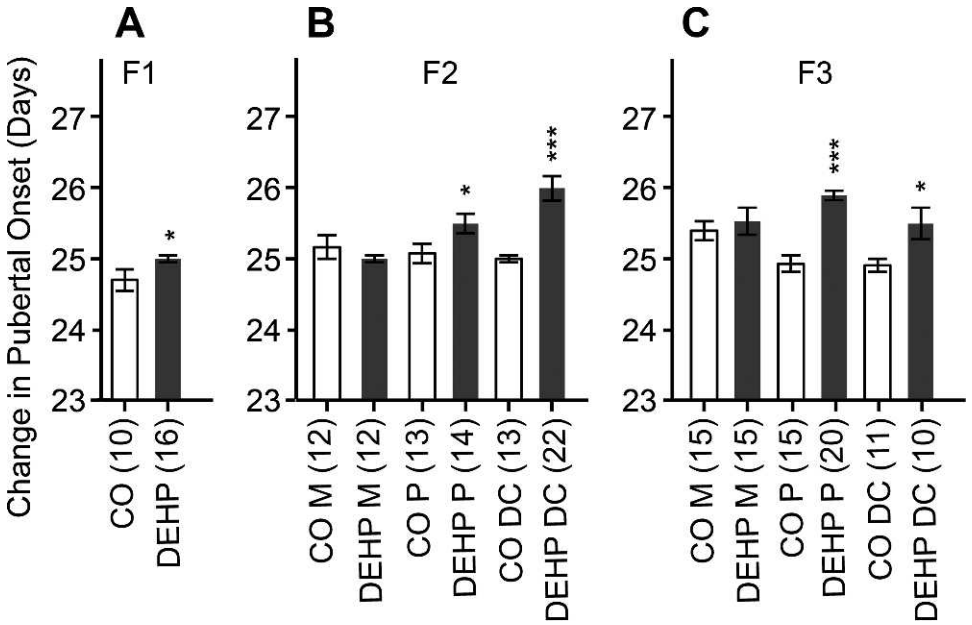


FIG. 2. Male pubertal onset of F1, F2, and F3 male offspring. The age of male pups was noted when prepuce detachment occurred. The average age of pubertal onset for F1, F2, and F3 male offspring in the vehicle control group was P24.7. Changes in days of the pubertal onset for F1 (**A**), F2 (**B**), and F3 (**C**) male pups from the corn oil vehicle (CO) and DEHP groups for the maternal (M), paternal (P), and double-cross (DC) lines were graphed. The number (n) in the parentheses indicates the number of male offspring for the CO and DEHP groups. Values are mean ± SEM. Pooled *t*-tests were conducted for the control and DEHP values; ***$P < 0.001$, *$P < 0.05$, no asterisk indicates $P > 0.05$.

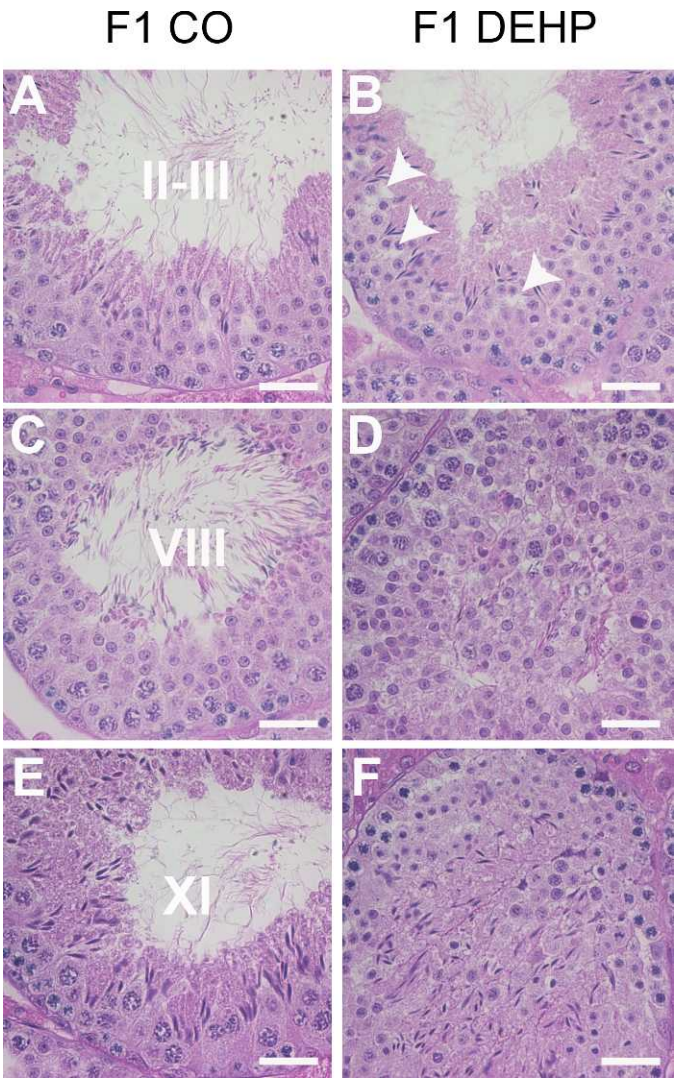


FIG. 3. Testicular cross sections from F1 offspring. Hematoxylin and eosin-stained testicular cross sections for F1 offspring at P120 after embryonic exposure to corn oil vehicle (CO; **A**, **C**, and **E**) and DEHP (**B**, **D**, and **F**). The stages of seminiferous epithelial cycle are noted in control sections (**A**, **C**, and **E**). Arrowheads indicate small vacuoles (**B**). Bar = 50 μm. Photomicrographs are representative of n ≥ 6 offspring for both the vehicle control and DEHP groups from two sets of embryonic exposures.

from DEHP- and corn oil vehicle-treated groups for all three breeding lines. The majority of the TUNEL-positive cells in the control group were located near the basement membrane (Fig. 7A), whereas the TUNEL-positive cells in the DEHP group were located near the basement membrane and also one layer above (Fig. 7, B and C). There were also tubules containing sloughed germ cells that did not have any positive stain (Fig. 7C, arrow). The apoptotic tubules with four or more TUNEL-positive cells were counted. There were no statistically significant differences at $P < 0.05$ for the F1 offspring from the DEHP-treated group (Fig. 7D) or the F2 and F3 offspring from the DEHP-treated group of all three breeding lines (Fig. 7, E and F). Thus, for DEHP treatment of F0 dams between E7 and E14 in mice, the germ cell disorganization observed in the F1, F2, and F3 offspring at P120 was independent of germ cell apoptosis. However, we cannot rule out that apoptosis did not occur earlier in the neonatal developmental window. Systematic developmental studies are necessary to determine if apoptosis contributed to DEHP-affected phenotypes.

### *DEHP Decreased Sperm Count and Motility in F2 and F3 Offspring*

To determine whether sperm count and motility changed transgenerationally, epididymal sperm from the F1, F2, F3, and F4 offspring at P120 of DEHP- and vehicle-treated groups were analyzed. There was a significant decrease in sperm count, on average 7.8% for F2, F3, and F4 offspring in all three lines (Fig. 8, B–D), except for the decrease in the sperm count for the maternal line for the F2 offspring, which was not significant at $P < 0.05$, but was close to significant ($P = 0.0594$). The F1 generation sperm counts had a decrease of 27.0%, more than 3-fold higher than those of the F2–F4 generations (Fig. 8A). This is not unexpected, because both germ cells and somatic cells of F1 embryos were directly exposed to DEHP. In terms of sperm motility, sperm from F1–F4 offspring of vehicle-treated F0 dams had a forward progressive motility at a frequency of 78.7% on average, whereas sperm from F1–F4 offspring of DEHP-treated F0 dams exhibited a forward progressive motility at a frequency of 53.0% on average, a decrease in motility compared to controls.

### *Stem Cell Function of F3 Offspring Is Impaired*

Recent reports that phthalates decreased the proliferation of the SSC line [41, 42] led to the investigation of SSC function. Germ cells from F3 offspring (P24 to P31) of the DEHP-treated group in the double-cross line and nontreated CD1 control mice were used as SSC donors and transplanted into $W/W^V$ recipient mice, which have no endogenous germ cells undergoing meiosis. Germ cells from F3 offspring were chosen for studying the transgenerational effects because they were not directly exposed to DEHP, whereas the germ cells in F2 offspring were derived from the primordial germ cells in the F1 offspring that were directly exposed to DEHP. The weights of testes from P30 animals in the control and DEHP groups from the F3 generation were not significantly different at $P < 0.05$ (data not shown).

The hematoxylin and eosin-stained testis cross sections from the $W/W^V$ recipients injected with nontreated control CD1 germ cells revealed the presence of seminiferous tubules containing germ cells (Fig. 9A), a 65.1% donor germ cell-derived recovery (Fig. 9J). In contrast, the testis cross sections of $W/W^V$ recipients injected with germ cells from F3 offspring of the DEHP-treated group displayed a dramatic decrease in tubules containing donor-derived germ cells (Fig. 9B, arrows), a 4.7% recovery (7.3% of the control) (Fig. 9J). Anti-DDX4 antibody immunostaining (examples shown in Fig. 9, D–F) and anti-γH2AX antibody immunostaining (examples shown in Fig. 9, G–I) and counting (Fig. 9, K and L) confirmed that there are fewer tubules with meiotic and postmeiotic germ cells. DDX4 is found in spermatogonia and spermatocytes, as well as in spermatids, staining more than two layers of germ cells [43]; γH2AX is localized to preleptotene, leptotene, zygotene, and early pachytene spermatocytes in the testis [44]. As an endogenous negative control, noninjected $W/W^V$ testes were used. Noninjected $W/W^V$ testes did not contain any donor-derived germ cells (Fig. 9C) and anti-γH2AX (Fig. 9I) immunostains did not reveal any immune-positive cells.

To further examine if the recovered tubules had a complete spermatogenesis, the recovered tubules were counted for the presence of round or elongated spermatids. In the $W/W^V$ recipients injected with control CD1 germ cells, 53.3% and 55.6% of the tubules contained round and elongated spermatids, respectively (Fig. 9, M and N). In contrast, there was a dramatic decrease in round and elongated spermatids in the W/

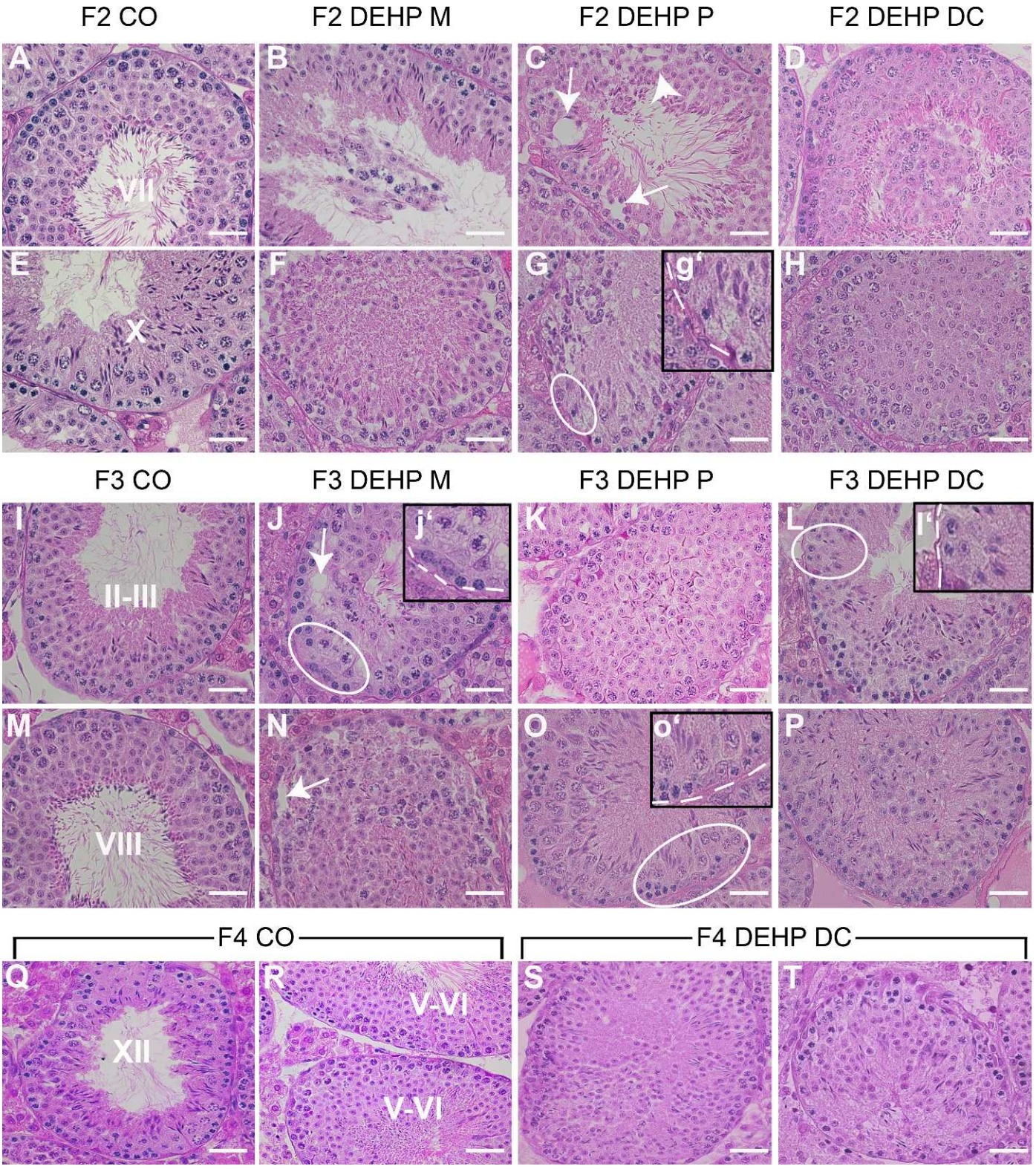


FIG. 4. Testicular cross sections from F2, F3, and F4 offspring at P120. Hematoxylin and eosin-stained testicular cross sections for the F2 and F3 offspring at P120 in the control vehicle group (CO; **A**, **E**, **I**, and **M**) and DEHP group in the maternal (M; **B**, **F**, **J**, and **N**), paternal (P; **C**, **G**, **K**, and **O**), and double-cross (DC; **D**, **H**, **L**, and **P**) lines and for the F4 offspring at P120 in the control vehicle group (**Q** and **R**) and DEHP group (**S** and **T**) in the double-cross line (DC) are shown. The stages of seminiferous epithelial cycle are noted in control sections (**A**, **E**, **I**, **M**, **Q**, and **R**). Arrowheads indicate areas where small vacuoles were observed. Arrows indicate areas where large vacuoles were observed. Oblong circles are magnified in **g‘**, **j‘**, **l‘**, and **o‘**, showing areas with germ cells missing. Bar = 50 μm. Photomicrographs are representative of $n \geq 6$ offspring for the F2 and F3 generations and three breeding lines from two sets of embryonic exposures and $n \geq 3$ offspring for the F4 generation.

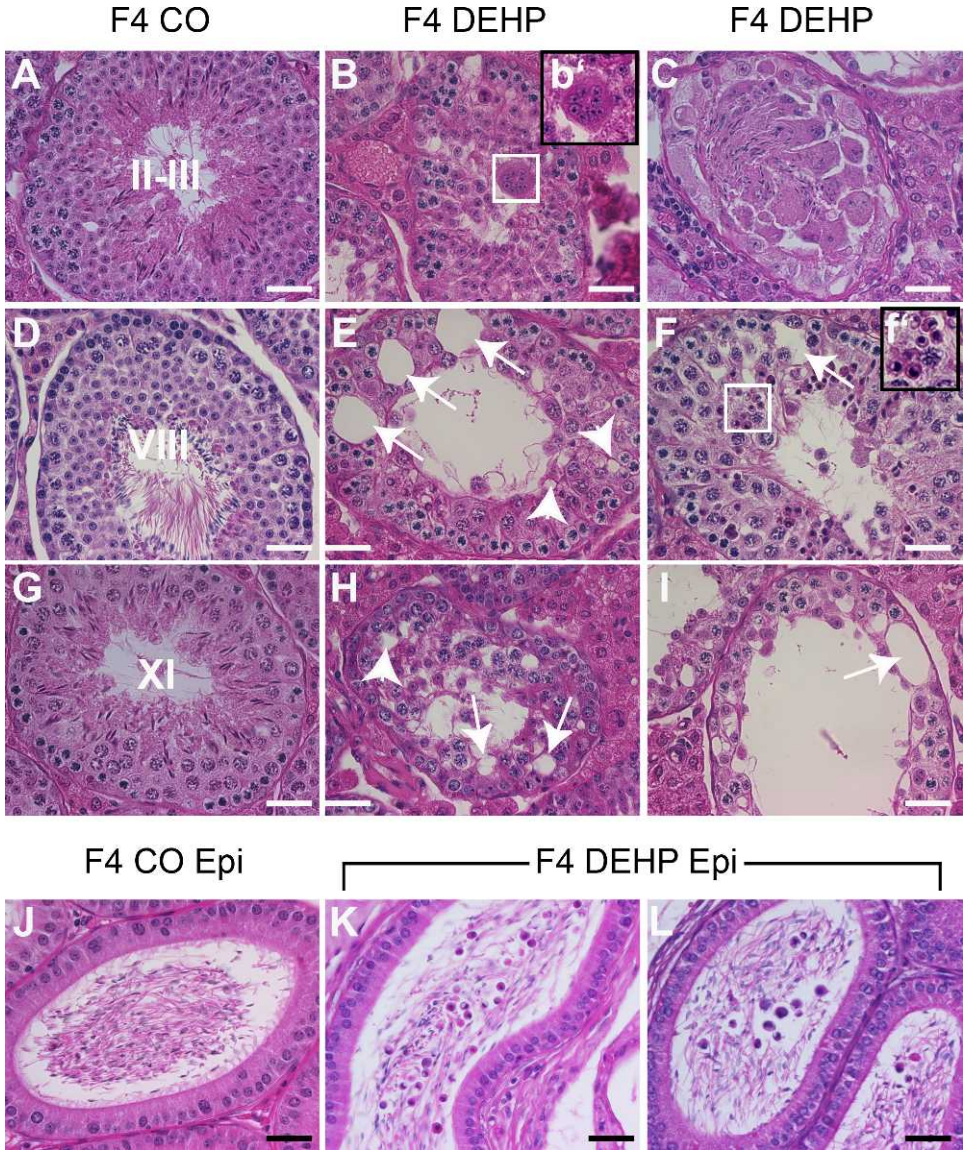


FIG. 5. Testicular and epididymal cross sections from F4 offspring at P360. Hematoxylin and eosin-stained testicular and epididymal cross sections for the F4 offspring at P360 in the control vehicle group (CO; **A**, **D**, and **G**) and DEHP group in the double-cross line (DC; **B**, **C**, **E**, **F**, **H**, and, **I**) are shown. The stages of seminiferous epithelial cycle are noted in control sections (**A**, **D**, and **G**). Arrowheads indicate areas where small vacuoles were observed. Arrows indicate areas where large vacuoles were observed. Boxed areas are magnified in **b′** and **f′**, showing multinucleated cells. Hematoxylin and eosin-stained epididymal cauda cross sections for the F4 offspring at P360 in the CO group (**J**) and DEHP group (**K** and **L**). Bar = 50 μm. Photomicrographs are representative of n ≥ 3 offspring.

$W^V$ recipients injected with F3 offspring germ cells from the DEHP-treated group, with only 4.5% (8.4% of the control) of the tubules containing round spermatids and 1.8% (3.2% of the control) of the tubules containing elongated spermatids (Fig. 9, M and N).

### *Stem Cells from F3 Offspring of the DEHP-Treated Group Have Decreased Colonization*

To determine if there was any difference in the number of undifferentiated spermatogonia in the $W/W^V$ recipient testes, anti-DMRT1 antibody was used. Anti-DMRT1 strongly immunostains undifferentiated spermatogonia (white arrows in Fig. 10, A, B, and C) and lightly stains differentiated spermatogonia and Sertoli cells [45]. Tubules containing the brightest-staining undifferentiated spermatogonia were counted in the $W/W^V$ recipients injected with control germ cells, in F3 germ cells from the DEHP group, and in the noninjected $W/W^V$ testes. The $W/W^V$ control recipients injected with untreated CD1 donor cells had 58.6% of tubules with undifferentiated spermatogonia (Fig. 10I), whereas the $W/W^V$ recipients injected with F3 DEHP donor cells had 12.2% of tubules with undifferentiated spermatogonia (20.8% of the control). Thus, these results indicate that a large decrease (~79%) in stem cell colonization compared to the controls.

The recipient testes were further examined for tubules that contained differentiating spermatogonia and early meiotic spermatocytes. The antibody against stimulated by retinoic acid gene 8 (STRA8) was chosen to examine cell types (represented by darkly staining brown nuclei), differentiating spermatogonia (A1–A4, Int, and B) and early meiotic spermatocytes (preleptotene and leptotene) [46]. The $W/W^V$ control recipients injected with untreated CD1 donor cells had 46.3% of tubules with differentiated spermatogonia and early

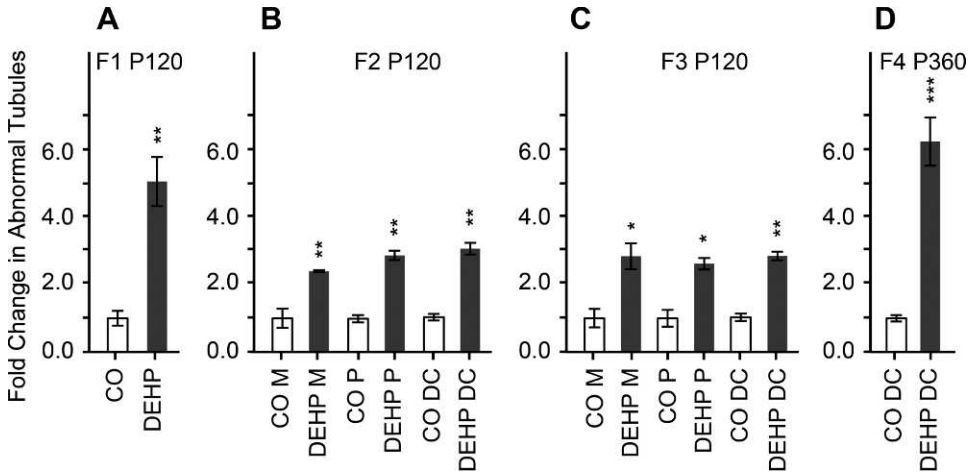


FIG. 6. Fold changes in abnormal tubules for F1–F3 offspring at P120 and F4 offspring at P360. Moderately and severely disorganized seminiferous tubules were counted and the percentage abnormality calculated by counting the total number of tubules on three or four sections spaced 50 μm apart per testis from n ≥ 3 offspring (≥9–12 sections). The fold change for the DEHP group was calculated by the percentage average of abnormal tubules in the control vehicle group (CO) set to 1. The fold changes in abnormal tubules were graphed for the F1 offspring at P120 (**A**); for the F2 and F3 offspring at P120 from the maternal (M), paternal (P), and double-cross (DC; **B** and **C**) lines; and for the F4 offspring at P360 from DC (**D**). Fold change values are means ± SEM. Pooled *t*-tests were conducted for the control and DEHP values; ***$P < 0.001$, **$P < 0.01$, *$P < 0.05$, no asterisk indicates $P > 0.05$.

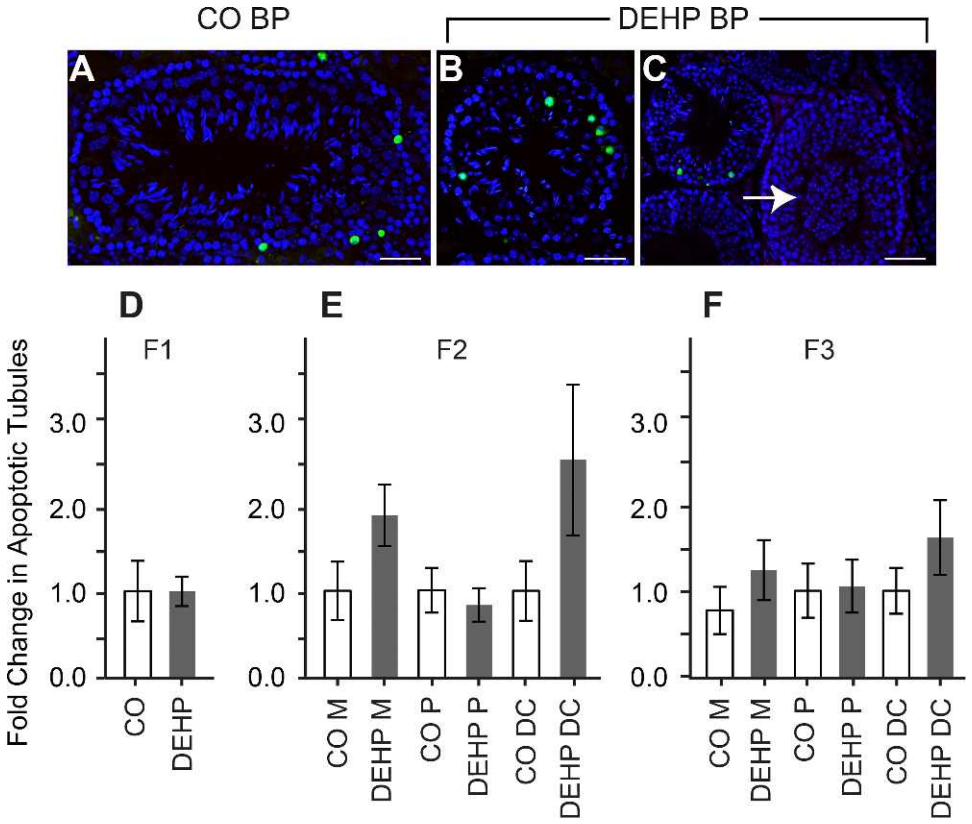


FIG. 7. Fold changes in apoptotic tubules in F1–F3 offspring at P120. TUNEL assay was performed on three or four sections spaced 50 μm apart per testis from n ≥ 3 offspring (≥9–12 sections). Tubules with four or more apoptotic cells and the total number of tubules were counted to calculate the percentage apoptosis. Examples of tubules with apoptotic cells for the control (**A**) and DEHP (**B** and **C**) groups are shown. Arrow in **C** indicates abnormal seminiferous tubule with sloughed germ cells and no TUNEL-positive cells. The fold change for DEHP group was calculated by the percentage average of apoptotic tubules in the control vehicle group (CO) set to 1. The fold changes in apoptotic tubules were graphed for the F1 offspring at P120 (**D**) and for the F2 and F3 offspring at P120 from the maternal (M), paternal (P), and double-cross (DC; **E** and **F**) lines. Fold change values are means ± SEM. Pooled *t*-tests were conducted for the control and DEHP values and there were no significant differences at $P < 0.05$. Bars in **A**–**C** = 100 μm.

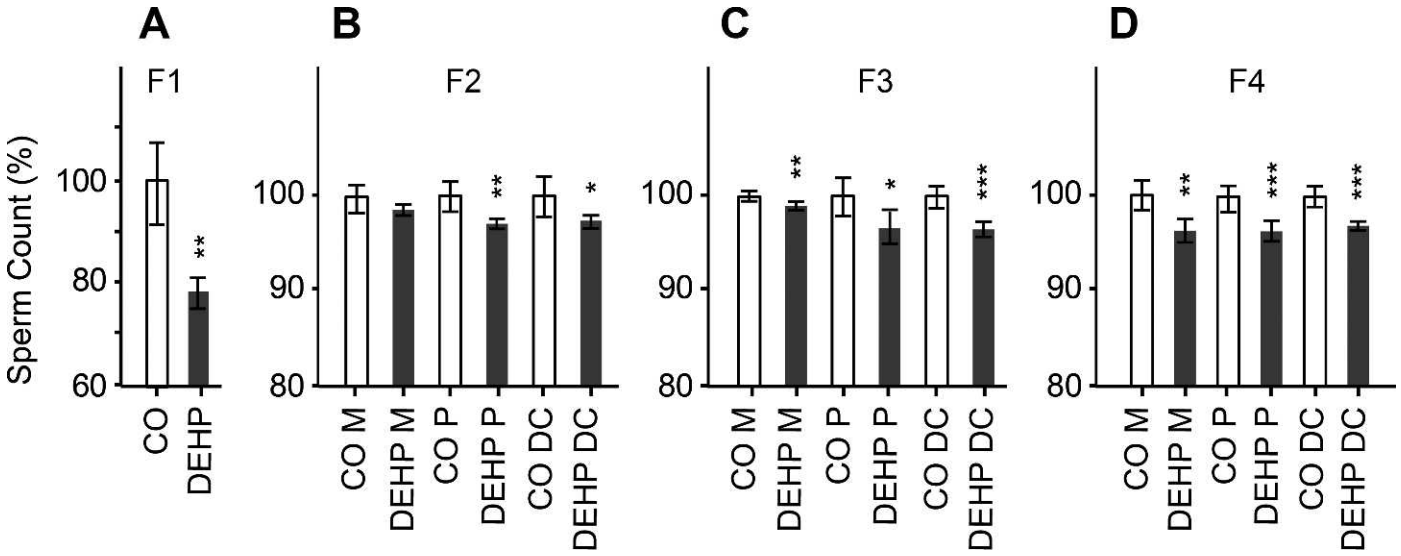


FIG. 8. Epididymal sperm count from F1–F4 offspring at P120. Epididymal sperm counts were performed on caudal sperm from n ≥ 6 offspring for the F1, F2, F3, and F4 generations. The percentage change in sperm count for DEHP group was calculated against the control group (CO) sperm count set to 100%. The percentage sperm count were graphed for the F1 (**A**), F2 (**B**), F3 (**C**) and F4 (**D**) offspring at P120 from the maternal (M), paternal (P), and double-cross (DC) lines. The percentage age values are means ± SEM. Pooled *t*-tests were conducted for the control and DEHP values; ***$P < 0.001$, **$P < 0.01$, *$P < 0.05$, no asterisk indicates $P > 0.05$.

meiotic spermatocytes expressing STRA8, whereas 8.9% of the tubules (19.5% of the control) in the recipient testes injected with F3 germ cells from the DEHP-treated group had STRA8-positive cells (Fig. 10J). Together, these results indicate that there was no further decrease in donor-derived spermatogenic cells after the initial large decrease in stem cell colonization and proliferation observed with the DMRT1 immunostaining. However, there was a second large drop in donor-derived spermatogenic cells from the beginning of meiosis (19.5% STRA8-positive cells) to the round spermatid stage (Fig. 9, 8.4% of control tubules with round spermatids).

### *Germ Cell Disorganization Is an Inherent Property of F3 Stem Cells from DEHP-Treated Group*

Interestingly, when the tubules from the $W/W^V$ recipients transplanted with the F3 offspring germ cells were examined, they had germ cell disorganization (Fig. 11, B, C, E, F, H, and I) very similar to the germ cell disorganization observed in testes from the F3 and F4 offspring of the DEHP-treated group at P120 and P360 (Figs. 4 and 5). The tubules appeared to lack layers of germ cells, were disorganized, and had areas where vacuoles were observed (Fig. 11B) or contained multinucleated cells (Fig. 11, C, F, and I, arrows). On the other hand, the tubules from the recipients injected with untreated CD1 germ cells had normal morphology with readily observable normal stages of seminiferous epithelium (Fig. 11, A, D, and G).

## DISCUSSION

DEHP is a known testicular toxicant and its effects on the rodent testis of F1 offspring after direct embryonic and lactational exposure have been widely documented [12–14, 17, 19, 20, 24]. We undertook this study to investigate the reproductive effects of DEHP exposure to F0 dams on the testis of progeny over multiple generations (F1–F4). We are reporting for the first time that the disruption of testicular function is not limited to the F1 offspring, but that abnormal testicular function persists in F2–F4 offspring. We found that DEHP exposure to F0 dams of CD1 outbred mouse strain at the E7–E14 window of gestation induced disruption of SSC colonization and proliferation and germ cell associations/organization in multiple generations, and, interestingly, the germ cell disorganization phenotype was an inherent property of SSCs of F3 offspring.

Specifically, we identified in the testes from the offspring at P120 of the DEHP-exposed dams increased testicular germ cell disorganization and a loss of identifiable stages of the seminiferous epithelial cycle (germ cell disorganization) in the F1–F4 generations. These acquired phenotypic traits were inherited through the maternal, paternal, and double-cross lines. The abnormal tubule morphology at P120 was observed on average at a frequency of 27.1% of total tubules in F2 and F3 offspring, and consisted of tubules with no lumen, tubules with a massive sloughing of germ cells blocking the lumen, tubules with missing germ cell types or layers of germ cells, and tubules with a complete loss of germ cell organization. It is not insignificant that these disorganized tubules were observed in F1–F4 offspring, because highly organized architecture of germ cell associations in the seminiferous epithelium is required for efficient and quantitative spermatogenesis, providing continuous production of sperm throughout the lifetime [47].

All germ cell types were present in the disorganized tubules and only a 7.8% decrease in sperm counts was detected for F2–F4 offspring at P120 in the paternal and double-cross lines. In the F1 generation, the decrease of 27.0% in sperm number was more than 3-fold higher than those for the F2–F4 generations. This higher percentage decrease in the F1 generation is not surprising, because germ cells and somatic cells in the F1 generation are directly exposed to DEHP. These sperm results are consistent with higher tubule abnormalities observed in the F1 generation (5.0-fold), comparing the control and DEHP-exposed group, and with tubule abnormalities (2.8- to 3.2-fold) persisting in the F2 and F3 generations.

Moreover, the testicular abnormalities were found to be progressively worse with aging (120–360 days), with an increased frequency (66.6% vs. 27.1%) and severity. The seminiferous tubule sections from F4 offspring at P360 had

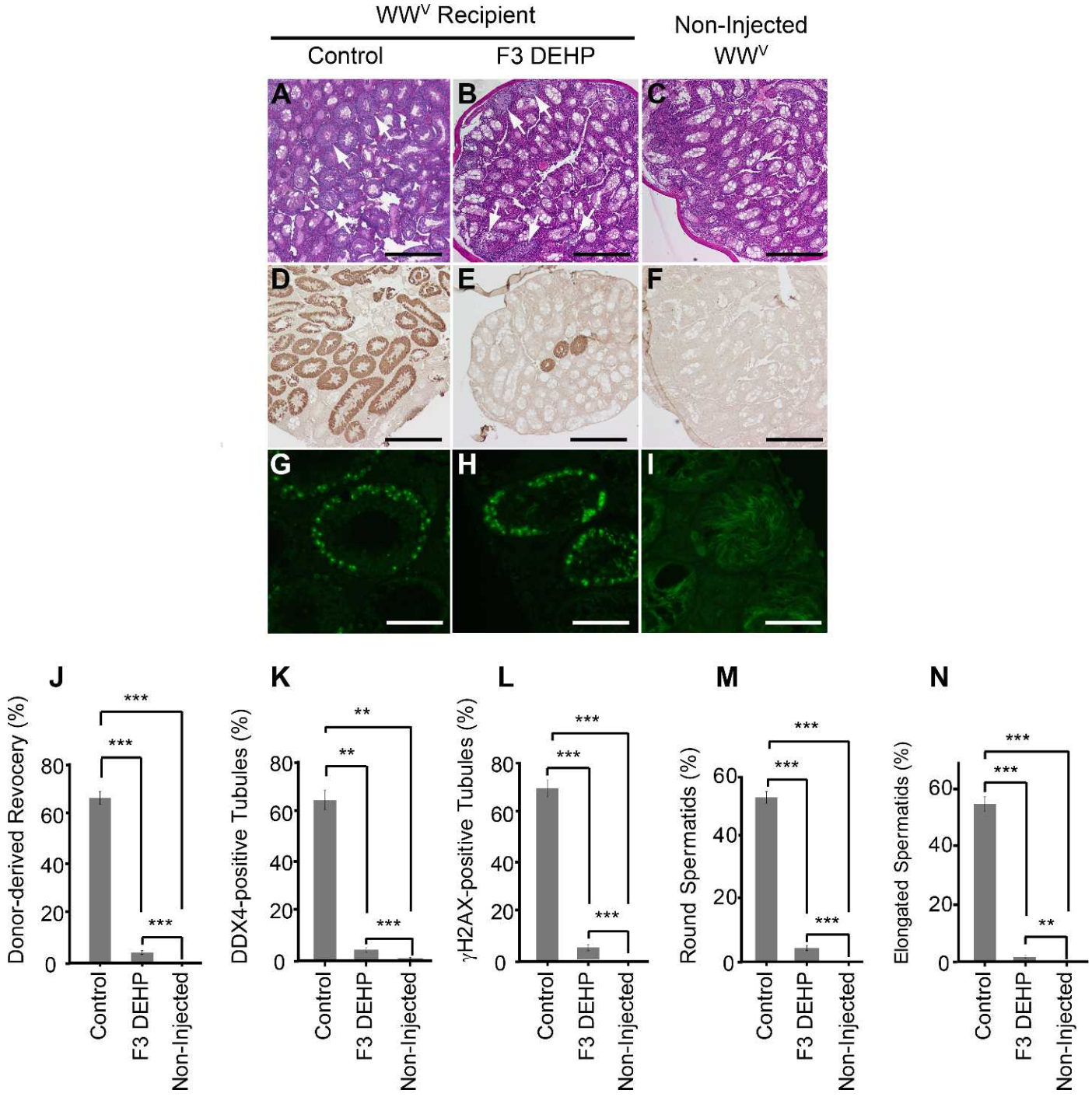


FIG. 9. W/W$^V$ recipient mice injected with donor germ cells from F3 offspring of DEHP-treated F0 dams. Testicular cross sections from W/W$^V$ recipients injected with germ cells from untreated CD1 control mice (**A**, **D**, and **G**), germ cells from F3 offspring derived from DEHP-exposed F0 dams (**B**, **E**, and **H**), and a noninjected W/W$^V$ control testis (**C**, **F**, and **I**) were stained with hematoxylin and eosin (**A**–**C**) or immunostained using anti-DDX4 antibody (**D**–**F**) or anti-γH2AX antibody (**G**–**I**). To quantify the extent of recovery, tubules containing donor-derived germ cells (**J**), tubules with 2 or more layers of anti-DDX4 immunostain (**K**), tubules with anti-γH2AX immunostain (**L**), tubules with round spermatids (**M**), and tubules with elongated spermatids (**N**) were counted and graphed. Values are means ± SEM for n ≥ 3 offspring and for two to six sections separated by 50 μm per testis. Pooled *t*-tests were conducted for the control and DEHP values; ***$P < 0.001$, **$P < 0.01$. Bars = 400 μm (**A**–**F**) and 50 μm (**G**–**I**). The negative controls showed no staining with only secondary antibody present, but without γH2AX or DDX4 primary antibodies (data not shown).

abnormal germ cell arrangements as seen in tubules from F4 offspring at P120, but also tubules with the germ cell layers missing and tubules with multinucleated cells. Although the length of treatment and treated rodent species were different, the abnormal testicular morphologies at P360 were similar to morphologies reported in previous studies, in which rat embryos were treated for a longer time, in utero and by lactation (for example, E8–P17 or E6–P21) [14, 19, 20]. However, our studies were unique in that the reproductive life span of offspring from the DEHP group seemed to decrease compared to that of the controls in a transgenerational manner. An age-related progressive increase in the incidence of the

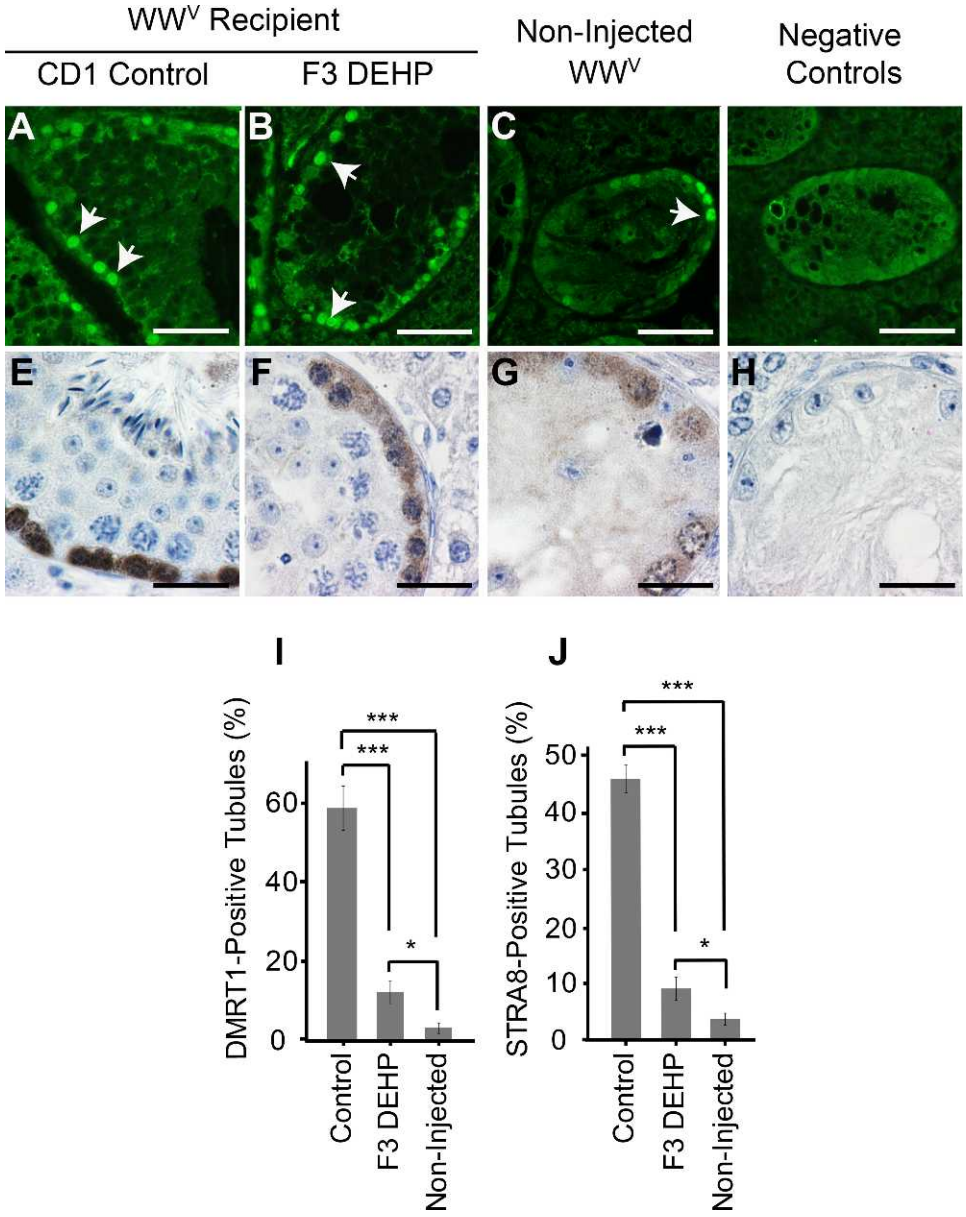


FIG. 10. W/W$^V$ recipient testicular tubules containing undifferentiated, differentiated, and premeiotic germ cells. Immunofluorescence and immunohistochemistry were performed using an anti-DMRT1 antibody (**A**–**D**) and an anti-STRA8 antibody (**E**–**H**), respectively, on testicular sections from W/W$^V$ mice injected with germ cells from untreated control CD1 mice (**A** and **E**) and germ cells from F3 offspring of DEHP-treated F0 dams (**B** and **F**), and noninjected W/W$^V$ control mice (**C** and **G**). Anti-DMRT1 antibody immunostains undifferentiated spermatogonia strongly (examples shown by brightly fluorescent cells marked by white arrowheads in **A**, **B**, and **C**). Using Adobe Photoshop CS (Adobe Systems Inc., San Jose, CA) the Alexa-555 color (red) was postprocessed to give a green color for better visualization. Anti-STRA8 antibody immunostains differentiated spermatogonia and premeiotic spermatocytes (examples indicated by brown stained cell nuclei in **E**, **F**, and **G**). Negative staining of the secondary antibody (negative controls) only on testis sections for anti-DMRT1 antibody and anti-STRA8 antibody did not show any staining (**D** and **H**). Bars = 50 μm (**A**–**D**) and 20 μm (**E**–**H**). Photomicrographs are representative of n $\geq$ 3 animals. To quantify, DMRT1-positive tubules containing brightly stained undifferentiated spermatogonia (**I**) and STRA8-positive tubules containing differentiated spermatogonia and premeiotic spermatocytes (**J**) were counted as well as the total tubules. Values are percentage means ± SEM from n $\geq$ 3 animals and two to six sections per testis spaced apart by 50 μm. Pooled *t*-tests were conducted for the control and DEHP values; ***$P < 0.001$, *$P < 0.05$ (**I** and **J**).

abnormal testicular phenotypes could be due to an age-related decline in Sertoli cell function in the testis from F3 offspring. Previously, it was shown that Sertoli cells were a target of phthalates [48], and a recent review indicated that the stem cell niche function dictated by testicular somatic cells declines with aging [49].

We hypothesize that germ cell disorganization phenotypes may result from the loss of molecular cues for cell-cell interactions important for setting up the germ cell associations of the seminiferous epithelium cycle. Consistent with this, it was reported previously that MEHP disrupted junctional complexes between Sertoli cells, and between Sertoli cells and germ cells, in C57BL/6 mice at P28 [50]. This paper also showed that MEHP-mediated germ cell detachment from Sertoli cells was not dependent on germ cell apoptosis, similar to our results. Further systematic investigation is required to determine the molecular cues altered by in utero DEHP treatment that can control the proper cell-cell interactions in the testis of F3 offspring.

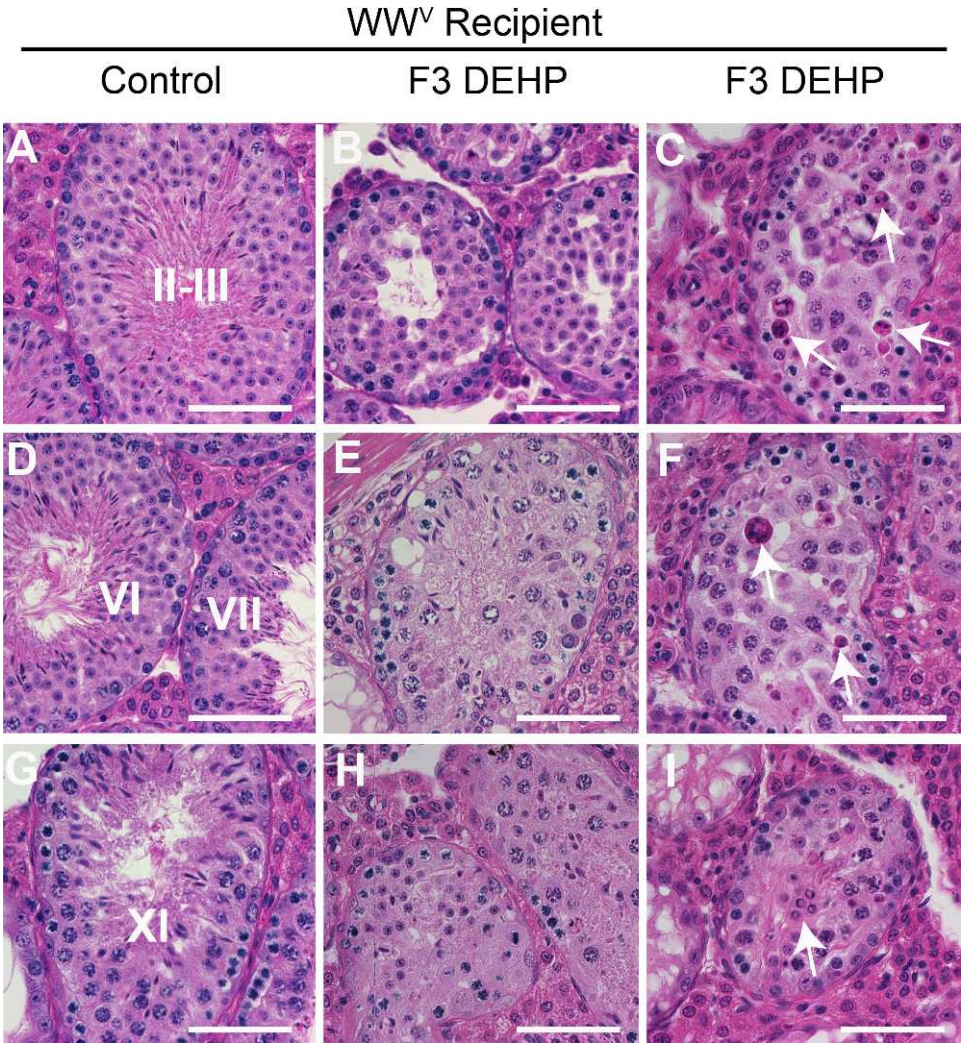


FIG. 11. Morphology of recovered tubules in W/W$^V$ mice injected with germ cells from F3 offspring of DEHP-exposed F0 dams. Testicular cross sections from W/W$^V$ recipients injected with germ cells from untreated CD1 control mice (**A**, **D**, and **G**), showing normal stages of seminiferous epithelium, and germ cells from F3 offspring from DEHP-exposed F0 dams (**B**, **C**, **E**, **F**, **H**, and **I**), showing abnormal testicular morphology such that the stages of the seminiferous epithelium could not be assigned. Arrows indicate multinucleated cells. Bar = 50 μm. Photomicrographs are representative of n ≥ 3 animals.

Recently, albeit in a cell line, it was shown that MEHP decreased the SSC proliferation in the C18-4 SSC-derived cell line by disrupting glial cell-derived neurotrophic factor (GDNF) signaling [41, 42]. Using the spermatogonial transplantation assay, we found a dramatic decrease (92.7%) in the tubules containing donor-derived meiotic/postmeiotic germ cells in the recipients injected with F3 germ cells from the DEHP-exposed group compared to the recipients injected with control germ cells. Moreover, using the markers of undifferentiated and differentiated spermatogonia, DMRT1 and STRA8, respectively, we detected that the first major block in the donor-derived spermatogenesis (79% decrease) was before the appearance of undifferentiated spermatogonia, perhaps in SSC colonization and initial proliferation of undifferentiated spermatogonia. In normal neonatal testis, the migration of gonocytes to the basement membrane to become stem cells may be affected by phthalates. Supportive of this, gonocytes at P3 in rats were shown to be sensitive to MEHP in organ cultures [21, 51]. Also supportive is a recent report that MEHP decreased the expression of β1-integrin expression in the testis [50], and the loss of function of β1-integrin signaling in germ cells and Sertoli cells has been linked to a loss of SSC homing to the stem cell niche in the testis [52]. However, we cannot rule out that the number of stem cells in the germ cell population that we transplanted was also less in F3 offspring in the DEHP group compared to the control. Further analysis is needed to sort out different possibilities. Nonetheless, these results are important in that in utero DEHP exposure in F0 dams affected the germ line at the level of the SSC function transgenerationally. Our analyses further indicated that there was a second block going through meiosis, from 19.5% of tubules containing differentiated spermatogonia and early meiotic spermatocytes to 8.4% of tubules containing round spermatids, which also should be followed in future analysis.

Moreover, it was remarkable that the recovered tubules from F3 germ cells of the DEHP group after transplantation had testicular morphologies replicating what was observed in the abnormal tubules at P120 and P360. These results showed that transgenerationally acquired testicular phenotypes observed in F3 offspring after the embryonic exposure to DEHP of the F0 dams were derived from the changed property of SSCs of F3 offspring. These findings are similar to observations made after transplantation of GDNF- [53] and WNT4-overexpressing [54] SSCs, where the phenotypes observed in the original donor testes was recapitulated in the transplanted testes. In the latter case, similar to our experiments, they also showed that the

progressive germ cell disorganization phenotype observed in the donor knockout testis was due to the loss of SSC function.

Our results showed that in utero exposure of DEHP to F0 dams reduced male AGDs, increased male nipple retention, and delayed pubertal onset in the F1 generation. This is similar to the results obtained in rats after embryonic and lactational exposure to DEHP [12–14, 19, 20]. Because fetal testicular testosterone synthesis is initiated at E12.5 in mice [55], DEHP could have changed fetal induction of steroidogenesis and changed AGD and nipple retention in F1 offspring. Neither decreased AGD nor male nipple retention traits observed in F1 offspring were transmitted to the F2 and F3 offspring. Interestingly, similar results were observed for in utero treatment of rats with antiandrogen flutamide [56]. Flutamide induced testicular degeneration and decreased sperm counts in F1 offspring, but the effects were not transmitted to F2 and F3 offspring, which led the investigators to conclude that an antiandrogenic mechanism was not transgenerational.

The exact molecular mechanism by which DEHP is able to disrupt the testis function transgenerationally remains unknown. DNA methylation changes that can be transmitted to the next generation as an epigenetic mechanism are of particular interest to us because the window of treatment (E7–E14) of this study included the time of global DNA demethylation for both male and female germ cells and remethylation of male germ cells [57]. DEHP could interfere with global demethylation and this could leave some DNA with methyl groups still attached. DEHP has been found to increase the methylation status of testicular genes and expression of DNA methyltransferases after E12.5 to E19 exposure [58]. Additionally, multiple lines of evidence strongly suggest that germ line epigenetic changes are inherited to future progeny generations in reproductive disorders, neuronal diseases, and cancer [27, 30, 59–61].

In conclusion, we report that DEHP-induced testicular germ cell disorganization and impaired SSC function passed from generation to generation and that the germ cell disorganization phenotypes were inherent to SSCs. Further work is needed to determine exactly what genes are methylated after embryonic exposure to DEHP, but not in controls, and how germ line epigenetic changes may be responsible for SSC colonization and establishment and maintenance of germ cell associations in future generation. The transgenerational effect of DEHP and other phthalates on humans is completely unknown, but evidence is mounting that links the levels of DEHP and its metabolites to reproductive disorders in those directly exposed and their offspring [5, 9, 10]. From this perspective, continued molecular work with DEHP and other endocrine disruptors is needed to shed new light on the potential risks of these compounds to disrupt reproductive outcomes over multiple generations.

## ACKNOWLEDGMENT

The authors thank Dr. Jannette Dufour (Texas Tech University) and Dr. Qien Yang (Washington State University) for their valuable input and critical reading of our manuscript. We thank Kelsey Brooks for her technical assistance. We also thank Dr. Michael Griswold (Washington State University) for the gift of the anti-STRA8 antibody and Dr. David Zarkower (University of Minnesota) for the gift of the anti-DMRT1 antibody.

## REFERENCES

1. Halden RU. Plastics and health risks. Annu Rev Public Health 2010; 31: 179–194.
2. CERHR. NTP-CERHR Monograph on the Potential Human Reproductive and Developmental Effects of Di (Ethylhexyl) Phthalate (DEHP). Research Triangle Park, North Carolina: National Institutes of Health; 2006:i–III76.
3. Silva MJ, Barr DB, Reidy JA, Malek NA, Hodge CC, Caudill SP, Brock JW, Needham LL, Calafat AM. Urinary levels of seven phthalate metabolites in the U.S. population from the National Health and Nutrition Examination Survey (NHANES) 1999–2000. Environ Health Perspect 2004; 112:331–338.
4. Koch HM, Calafat AM. Human body burdens of chemicals used in plastic manufacture. Philos Trans R Soc Lond B Biol Sci 2009; 364:2063–2078.
5. Hauser R, Meeker JD, Singh NP, Silva MJ, Ryan L, Duty S, Calafat AM. DNA damage in human sperm is related to urinary levels of phthalate monoester and oxidative metabolites. Hum Reprod 2007; 22:688–695.
6. Lambrot R, Muczynski V, Lecureuil C, Angenard G, Coffigny H, Pairault C, Moison D, Frydman R, Habert R, Rouiller-Fabre V. Phthalates impair germ cell development in the human fetal testis in vitro without change in testosterone production. Environ Health Perspect 2009; 117:32–37.
7. Desdoits-Lethimonier C, Albert O, Le Bizec B, Perdu E, Zalko D, Courant F, Lesne L, Guille F, Dejucq-Rainsford N, Jegou B. Human testis steroidogenesis is inhibited by phthalates. Hum Reprod 2012; 27: 1451–1459.
8. Main KM, Mortensen GK, Kaleva MM, Boisen KA, Damgaard IN, Chellakooty M, Schmidt IM, Suomi AM, Virtanen HE, Petersen DV, Andersson AM, Toppari J, et al. Human breast milk contamination with phthalates and alterations of endogenous reproductive hormones in infants three months of age. Environ Health Perspect 2006; 114:270–276.
9. Swan SH, Main KM, Liu F, Stewart SL, Kruse RL, Calafat AM, Mao CS, Redmon JB, Ternand CL, Sullivan S, Teague JL. Decrease in anogenital distance among male infants with prenatal phthalate exposure. Environ Health Perspect 2005; 113:1056–1061.
10. Marsee K, Woodruff TJ, Axelrad DA, Calafat AM, Swan SH. Estimated daily phthalate exposures in a population of mothers of male infants exhibiting reduced anogenital distance. Environ Health Perspect 2006; 114:805–809.
11. Skakkebaek NE, Rajpert-De Meyts E, Main KM. Testicular dysgenesis syndrome: an increasingly common developmental disorder with environmental aspects. Hum Reprod 2001; 16:972–978.
12. Moore RW, Rudy TA, Lin TM, Ko K, Peterson RE. Abnormalities of sexual development in male rats with in utero and lactational exposure to the antiandrogenic plasticizer di(2-ethylhexyl) phthalate. Environ Health Perspect 2001; 109:229–237.
13. Mylchreest E, Sar M, Cattley RC, Foster PM. Disruption of androgen-regulated male reproductive development by di(n-butyl) phthalate during late gestation in rats is different from flutamide. Toxicol Appl Pharmacol 1999; 156:81–95.
14. Parks LG, Ostby JS, Lambright CR, Abbott BD, Klinefelter GR, Barlow NJ, Gray LE Jr. The plasticizer diethylhexyl phthalate induces malformations by decreasing fetal testosterone synthesis during sexual differentiation in the male rat. Toxicol Sci 2000; 58:339–349.
15. Culty M, Thuillier R, Li W, Wang Y, Martinez-Arguelles DB, Benjamin CG, Triantafilou KM, Zirkin BR, Papadopoulos V. In utero exposure to di-(2-ethylhexyl) phthalate exerts both short-term and long-lasting suppressive effects on testosterone production in the rat. Biol Reprod 2008; 78:1018–1028.
16. Lin H, Lian QQ, Hu GX, Jin Y, Zhang Y, Hardy DO, Chen GR, Lu ZQ, Sottas CM, Hardy MP, Ge RS. In utero and lactational exposures to diethylhexyl-phthalate affect two populations of Leydig cells in male Long-Evans rats. Biol Reprod 2009; 80:882–888.
17. Mahood IK, Scott HM, Brown R, Hallmark N, Walker M, Sharpe RM. In utero exposure to di(n-butyl) phthalate and testicular dysgenesis: comparison of fetal and adult end points and their dose sensitivity. Environ Health Perspect 2007; 115(suppl 1):55–61.
18. Lague E, Tremblay JJ. Antagonistic effects of testosterone and the endocrine disruptor mono-(2-ethylhexyl) phthalate on INSL3 transcription in Leydig cells. Endocrinology 2008; 149:4688–4694.
19. Andrade AJ, Grande SW, Talsness CE, Gericke C, Grote K, Golombiewski A, Sterner-Kock A, Chahoud I. A dose response study following in utero and lactational exposure to di-(2-ethylhexyl) phthalate (DEHP): reproductive effects on adult male offspring rats. Toxicology 2006; 228: 85–97.
20. Gray LE Jr, Barlow NJ, Howdeshell KL, Ostby JS, Furr JR, Gray CL. Transgenerational effects of di (2-ethylhexyl) phthalate in the male CRL:CD(SD) rat: added value of assessing multiple offspring per litter. Toxicol Sci 2009; 110:411–425.
21. Li LH, Jester WF Jr, Laslett AL, Orth JM. A single dose of di-(2-ethylhexyl) phthalate in neonatal rats alters gonocytes, reduces Sertoli cell proliferation, and decreases cyclin D2 expression. Toxicol Appl Pharmacol 2000; 166:222–229.

22. Lehraiki A, Racine C, Krust A, Habert R, Levacher C. Phthalates impair germ cell number in the mouse fetal testis by an androgen- and estrogen-independent mechanism. Toxicol Sci 2009; 111:372–382.
23. Gaido KW, Hensley JB, Liu D, Wallace DG, Borghoff S, Johnson KJ, Hall SJ, Boekelheide K. Fetal mouse phthalate exposure shows that Gonocyte multinucleation is not associated with decreased testicular testosterone. Toxicol Sci 2007; 97:491–503.
24. Klinefelter GR, Laskey JW, Winnik WM, Suarez JD, Roberts NL, Strader LF, Riffle BW, Veeramachaneni DN. Novel molecular targets associated with testicular dysgenesis induced by gestational exposure to diethylhexyl phthalate in the rat: a role for estradiol. Reproduction 2012; 144:747–761.
25. Anway MD, Cupp AS, Uzumcu M, Skinner MK. Epigenetic transgenerational actions of endocrine disruptors and male fertility. Science 2005; 308:1466–1469.
26. Burdge GC, Hoile SP, Uller T, Thomas NA, Gluckman PD, Hanson MA, Lillycrop KA. Progressive, transgenerational changes in offspring phenotype and epigenotype following nutritional transition. PLoS One 2011; 6:e28282.
27. Manikkam M, Guerrero-Bosagna C, Tracey R, Haque MM, Skinner MK. Transgenerational actions of environmental compounds on reproductive disease and identification of epigenetic biomarkers of ancestral exposures. PLoS One 2012; 7:e31901.
28. Salian S, Doshi T, Vanage G. Perinatal exposure of rats to bisphenol A affects fertility of male offspring—an overview. Reprod Toxicol 2011; 31: 359–362.
29. Bruner-Tran KL, Osteen KG. Developmental exposure to TCDD reduces fertility and negatively affects pregnancy outcomes across multiple generations. Reprod Toxicol 2011; 31:344–350.
30. Guerrero-Bosagna C, Covert TR, Haque MM, Settles M, Nilsson EE, Anway MD, Skinner MK. Epigenetic transgenerational inheritance of vinclozolin induced mouse adult onset disease and associated sperm epigenome biomarkers. Reprod Toxicol 2012; 34:694–707.
31. Mohamed el SA, Song WH, Oh SA, Park YJ, You YA, Lee S, Choi JY, Kim YJ, Jo I, Pang MG. The transgenerational impact of benzo(a)pyrene on murine male fertility. Hum Reprod 2010; 25:2427–2433.
32. Pocar P, Fiandanese N, Secchi C, Berrini A, Fischer B, Schmidt JS, Schaedlich K, Rhind SM, Zhang Z, Borromeo V. Effects of polychlorinated biphenyls in CD-1 mice: reproductive toxicity and intergenerational transmission. Toxicol Sci 2012; 126:213–226.
33. Kalfa N, Paris F, Soyer-Gobillard MO, Daures JP, Sultan C. Prevalence of hypospadias in grandsons of women exposed to diethylstilbestrol during pregnancy: a multigenerational national cohort study. Fertil Steril 2011; 95:2574–2577.
34. Painter RC, Osmond C, Gluckman P, Hanson M, Phillips DI, Roseboom TJ. Transgenerational effects of prenatal exposure to the Dutch famine on neonatal adiposity and health in later life. BJOG 2008; 115:1243–1249.
35. Titus-Ernstoff L, Troisi R, Hatch EE, Hyer M, Wise LA, Palmer JR, Kaufman R, Adam E, Noller K, Herbst AL, Strohsnitter W, Cole BF, et al. Offspring of women exposed in utero to diethylstilbestrol (DES): a preliminary report of benign and malignant pathology in the third generation. Epidemiology 2008; 19:251–257.
36. Titus-Ernstoff L, Troisi R, Hatch EE, Palmer JR, Hyer M, Kaufman R, Adam E, Noller K, Hoover RN. Birth defects in the sons and daughters of women who were exposed in utero to diethylstilbestrol (DES). Int J Androl 2010; 33:377–384.
37. Durcova-Hills G, Capel B. Development of germ cells in the mouse. Curr Top Dev Biol 2008; 83:185–212.
38. Sharpe RM. ''Additional'' effects of phthalate mixtures on fetal testosterone production. Toxicol Sci 2008; 105:1–4.
39. Calafat AM, Brock JW, Silva MJ, Gray LE Jr, Reidy JA, Barr DB, Needham LL. Urinary and amniotic fluid levels of phthalate monoesters in rats after the oral administration of di(2-ethylhexyl) phthalate and di-n-butyl phthalate. Toxicology 2006; 217:22–30.
40. Doyle TJ, Braun KW, McLean DJ, Wright RW, Griswold MD, Kim KH. potential functions of retinoic acid receptor A in Sertoli cells and germ cells during spermatogenesis. Ann N Y Acad Sci 2008; 1120:114–130.
41. Lucas B, Fields C, Hofmann MC. Signaling pathways in spermatogonial stem cells and their disruption by toxicants. Birth Defects Res C Embryo Today 2009; 87:35–42.
42. Lucas BE, Fields C, Joshi N, Hofmann MC. Mono-(2-ethylhexyl)-phthalate (MEHP) affects ERK-dependent GDNF signalling in mouse stem-progenitor spermatogonia. Toxicology 2012; 299(1):10–19.
43. Toyooka Y, Tsunekawa N, Takahashi Y, Matsui Y, Satoh M, Noce T. Expression and intracellular localization of mouse Vasa-homologue protein during germ cell development. Mech Dev 2000; 93:139–149.
44. Blanco-Rodriguez J. gammaH2AX marks the main events of the spermatogenic process. Microsc Res Tech 2009; 72:823–832.
45. Matson CK, Murphy MW, Griswold MD, Yoshida S, Bardwell VJ, Zarkower D. The mammalian doublesex homolog DMRT1 is a transcriptional gatekeeper that controls the mitosis versus meiosis decision in male germ cells. Dev Cell 2010; 19:612–624.
46. Zhou Q, Nie R, Li Y, Friel P, Mitchell D, Hess RA, Small C, Griswold MD. Expression of stimulated by retinoic acid gene 8 (Stra8) in spermatogenic cells induced by retinoic acid: an in vivo study in vitamin A-sufficient postnatal murine testes. Biol Reprod 2008; 79:35–42.
47. Russell LD, Ettlin RA, Sinha Hikim AP, Clegg ED. The classification and timing of spermatogenesis. In: Histological and histopathological evaluation of the testis, 1 ed. Clearwater, FL: Cache River Press; 1990: 41–58.
48. Heindel JJ, Powell CJ. Phthalate ester effects on rat Sertoli cell function in vitro: effects of phthalate side chain and age of animal. Toxicol Appl Pharmacol 1992; 115:116–123.
49. Oatley JM, Brinster RL. The germline stem cell niche unit in mammalian testes. Physiol Rev 2012; 92:577–595.
50. Yao PL, Lin YC, Richburg JH. Mono-(2-ethylhexyl) phthalate-induced disruption of junctional complexes in the seminiferous epithelium of the rodent testis is mediated by MMP2. Biol Reprod 2010; 82:516–527.
51. Li H, Kim KH. Effects of mono-(2-ethylhexyl) phthalate on fetal and neonatal rat testis organ cultures. Biol Reprod 2003; 69:1964–1972.
52. Kanatsu-Shinohara M, Takehashi M, Takashima S, Lee J, Morimoto H, Chuma S, Raducanu A, Nakatsuji N, Fassler R, Shinohara T. Homing of mouse spermatogonial stem cells to germline niche depends on beta1-integrin. Cell Stem Cell 2008; 3:533–542.
53. Meng X, Lindahl M, Hyvonen ME, Parvinen M, de Rooij DG, Hess MW, Raatikainen-Ahokas A, Sainio K, Rauvala H, Lakso M, Pichel JG, Westphal H, et al. Regulation of cell fate decision of undifferentiated spermatogonia by GDNF. Science 2000; 287:1489–1493.
54. Boyer A, Yeh JR, Zhang X, Paquet M, Gaudin A, Nagano MC, Boerboom D. CTNNB1 signaling in Sertoli cells downregulates spermatogonial stem cell activity via WNT4. PLoS One 2012; 7:e29764.
55. Scott HM, Mason JI, Sharpe RM. Steroidogenesis in the fetal testis and its susceptibility to disruption by exogenous compounds. Endocr Rev 2009; 30:883–925.
56. Anway MD, Rekow SS, Skinner MK. Comparative anti-androgenic actions of vinclozolin and flutamide on transgenerational adult onset disease and spermatogenesis. Reprod Toxicol 2008; 26:100–106.
57. Mochizuki K, Matsui Y. Epigenetic profiles in primordial germ cells: global modulation and fine tuning of the epigenome for acquisition of totipotency. Dev Growth Differ 2010; 52:517–525.
58. Wu S, Zhu J, Li Y, Lin T, Gan L, Yuan X, Xiong J, Liu X, Xu M, Zhao D, Ma C, Li X, et al. Dynamic epigenetic changes involved in testicular toxicity induced by di-2-(ethylhexyl) phthalate in mice. Basic Clin Pharmacol Toxicol 2010; 106:118–123.
59. Bohacek J, Mansuy IM. Epigenetic inheritance of disease and disease risk. Neuropsychopharmacology 2013; 38:220–236.
60. Hitchins MP. Inheritance of epigenetic aberrations (constitutional epimutations) in cancer susceptibility. Adv Genet 2010; 70:201–243.
61. Nelson VR, Heaney JD, Tesar PJ, Davidson NO, Nadeau JH. Transgenerational epigenetic effects of the Apobec1 cytidine deaminase deficiency on testicular germ cell tumor susceptibility and embryonic viability. Proc Natl Acad Sci U S A 2012; 109:E2766–2773.